iScience

CellPress
OPEN ACCESS

Article

# Nicotinamide breaks effector CD8 T cell responses by targeting mTOR signaling

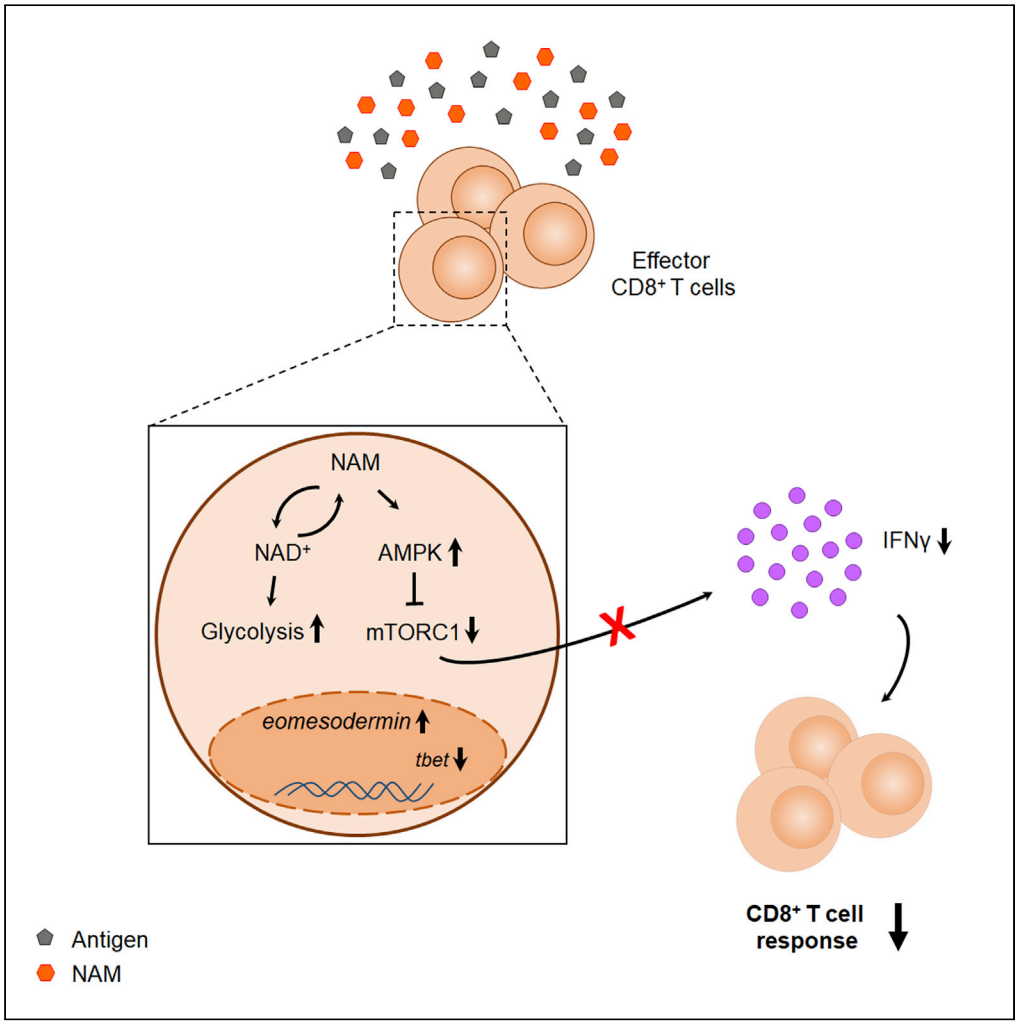


Federica Agliano, Timofey A. Karginov, Antoine Ménoret, Anthony Provatas, Anthony T. Vella

vella@uchc.edu

## Highlights

NAM increases glycolysis while reducing effector cytokine production

NAM inhibits mTORC1 activation

In T cells NAM induces the expression of memory markers

NAM diet supplementation modulates T cell effector potential *in vivo*

Agliano et al., iScience *25*, 103932
March 18, 2022 
https://doi.org/10.1016/j.isci.2022.103932

iScience

CellPress
OPEN ACCESS

Article

# Nicotinamide breaks effector CD8 T cell responses by targeting mTOR signaling

Federica Agliano,[1] Timofey A. Karginov,[1] Antoine Ménoret,[1] Anthony Provatas,[2] and Anthony T. Vella[1,3,*]

## SUMMARY

**Nicotinamide (NAM) shapes T cell responses but its precise molecular mechanism of action remains elusive. Here, we show that NAM impairs naive T cell effector transition but also effector T cells themselves. Although aerobic glycolysis is a hallmark of activated T cells, $CD8^+$ T cells exposed to NAM displayed enhanced glycolysis, yet producing significantly less IFNγ. Mechanistically, NAM reduced mTORC1 activity independently of $NAD^+$ metabolism, decreasing IFNγ translation and regulating T cell transcriptional factors critical to effector/memory fate. Finally, the role of NAM in a biomedically relevant model of lung injury was tested. Specifically, a NAM-supplemented diet reduced systemic IL-2, antigen-specific T cell clonal expansion, and effector function after inhalation of *Staphylococcus aureus* enterotoxin A. These findings identify NAM as a potential therapeutic supplement that uncouples glycolysis from effector cytokine production and may be a powerful treatment for diseases associated with T cell hyperactivation.**

## INTRODUCTION

Nicotinamide (NAM) is one of the three forms of vitamin B3, known as a precursor of nicotinamide adenine dinucleotide ($NAD^+$) (Bogan and Brenner, 2008; Rajman et al., 2018). Cellular content of NAM mainly derives from daily diet, such as poultry, beef, and fish; however, a recent study demonstrated gut microbiota as a potential alternative source of NAM for the host (Blacher et al., 2019). Lastly, NAM can also be formed from $NAD^+$ by $NAD^+$-consuming enzymes, such as sirtuins, poly-ADP-ribose polymerases (PARPs), and CD38 (Buque et al., 2021; Rajman et al., 2018). NAM has been reported to boost $NAD^+$ cellular content in several cell types (Hara et al., 2007; Rajman et al., 2018; Yu et al., 2020). In addition, it is now clear how NAM and other $NAD^+$ precursors can aid human health span in different scenarios such as nonmelanoma skin-cancers, systemic inflammation caused by heart failure and prediabetic female obesity (Chen et al., 2015; Rajman et al., 2018; Yoshino et al., 2021; Zhou et al., 2020), supporting the value of NAM as an efficacious dietary supplement.

Several studies have reported the *in vivo* anti-inflammatory effect of NAM (Mendez-Lara et al., 2021; Mitchell et al., 2018; Su et al., 2007). Consistent with these findings, NAM was shown to decrease inflammation and $CD4^+$ T cell infiltration in an Experimental Autoimmune Encephalitis (EAE) model (Kaneko et al., 2006); however, recent work demonstrated how NAM enhances T cell response and cytokine production, mediating chemopreventive effects in different models of murine cancers (Buque et al., 2020; Scatozza et al., 2020). Thus, the role of NAM in T cell-dependent immune responses has been seemingly contradictory. In addition, the molecular mechanism by which NAM shapes T cell function, and whether this is dependent on NAM conversion to $NAD^+$, remains largely unknown (Buque et al., 2021; Rajman et al., 2018). Thus, given the wide use of NAM as a dietary supplement and the tremendous contribution of T cell-mediated responses in diseases such as infections, cancer, and autoimmune disorders, it is imperative to understand how NAM exactly modulates T cell response and the molecular pathways involved.

Here, the role of NAM in T cells and its underlying mechanism of action were examined. Activated T cells display an enhanced glycolytic metabolism (Warburg effect) and glycolysis regulates IFNγ expression at an epigenetic and posttranscriptional level (Chang et al., 2013; Peng et al., 2016). We show that NAM modulates effector $CD8^+$ T cell metabolism and function, differentially regulating cell glycolytic potential and IFNγ release. Specifically, we uncovered a mechanism by which NAM inhibits the mechanistic target of rapamycin complex 1 (mTORC1) pathway, resulting in posttranscriptional control of IFNγ, and transcriptional

[1]Department of Immunology, School of Medicine, University of Connecticut, Farmington, CT 06030 USA

[2]Department of Chemistry, University of Connecticut, Storrs, CT 06269 USA

[3]Lead contact

*Correspondence: vella@uchc.edu

https://doi.org/10.1016/j.isci.2022.103932

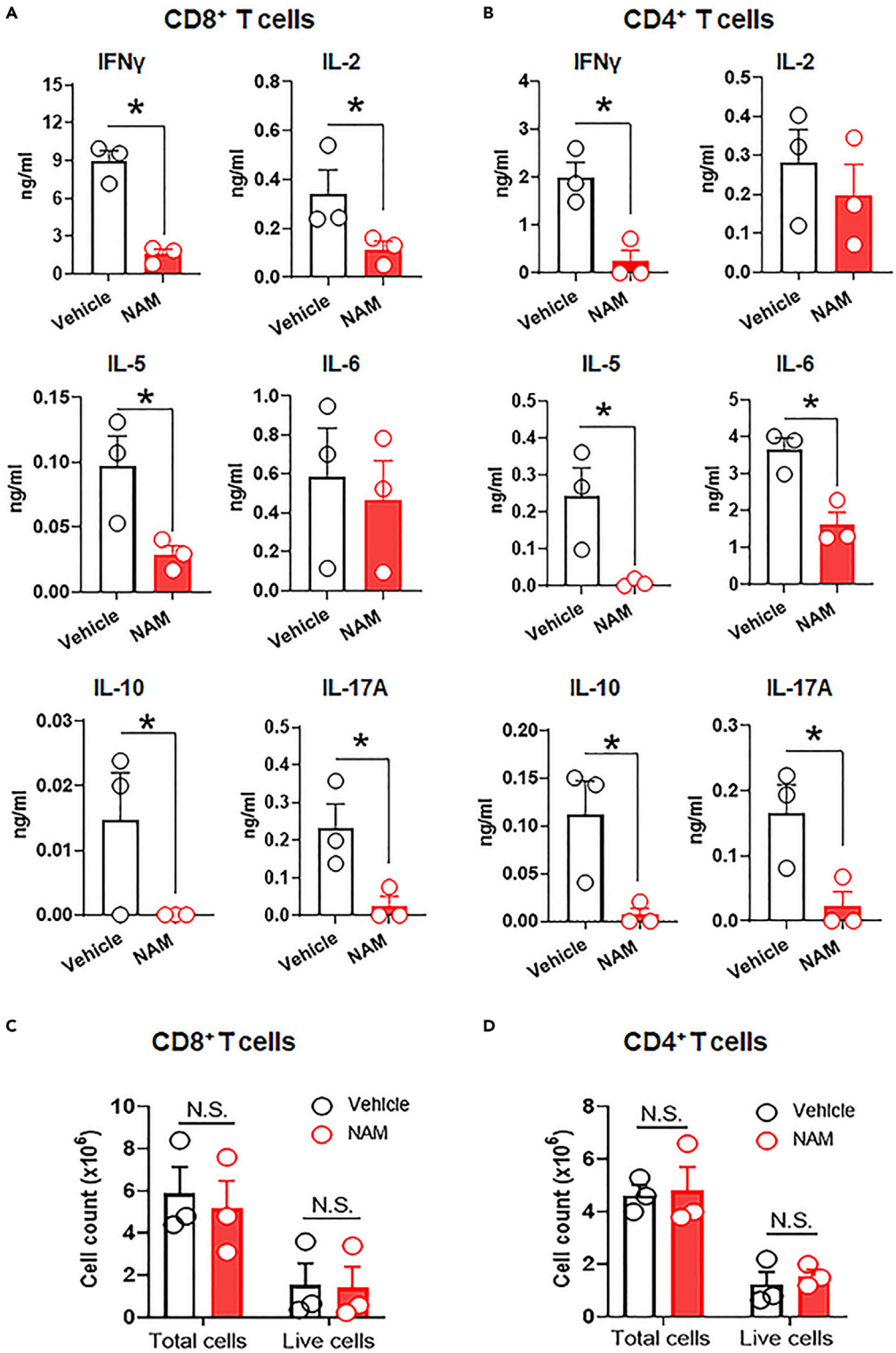


**Figure 1. NAM reduces cytokine production during effector T cell differentiation**

(A) Cytokine secretion of CD8$^+$ T cells activated *in vitro* with α-CD3/CD28 beads plus rhIL-2 (30 U/mL) for 66 h, with vehicle or NAM (10 mM).

(B) Cytokine secretion of CD4$^+$ T cells activated *in vitro* with α-CD3/CD28 beads plus rhIL-2 (30 U/mL) for 66 h, with vehicle or NAM (10 mM).

**Figure 1. *Continued***

(C) Cell count of negatively selected $CD8^+$ T cells activated *in vitro* with α-CD3/CD28 beads plus rhIL-2 (30 U/mL) for 66 h, with vehicle or NAM (10 mM). Numbers are given by counting cells before (total cells) and after (live cells) Lympholyte-M gradient.

(D) Cell count of negatively selected $CD4^+$ T cells activated *in vitro* with α-CD3/CD28 beads plus rhIL-2 (30 U/mL) for 66 h, with vehicle or NAM (10 mM). Numbers are given by counting cells before (total cells) and after (live cells) Lympholyte-M gradient. Each dot represents an independent experiment (n = 3-4 mice/experiment). Data are represented as mean ± SEM. *p <0.05, N.S. not significant by two-tailed unpaired t test. See also Figure S1.

regulation of effector/memory T cell markers. This T cell regulatory function is intrinsic to NAM, independent of its conversion to $NAD^+$. Consistent with these findings, we provide evidence that in a model of *Staphylococcus aureus* enterotoxin A inhalation, NAM food supplementation *in vivo* regulates T cell clonal expansion, and effector potential. *S. aureus* enterotoxin A induces powerful T cell-driven lung damage (Kumar et al., 2010; Muralimohan et al., 2008). Thus, our data reveal a precise mechanism of NAM controlling T cell function and suggest a potential effect of NAM dietary supplements as therapeutic intervention against T cell-mediated diseases.

## RESULTS

### NAM reduces cytokine production during effector T cell differentiation

Nicotinamide is generally known to decrease cytokine production and inflammatory responses in various cell types and tissues (Mendez-Lara et al., 2021; Rehman et al., 2021; Ungerstedt et al., 2003; Zheng et al., 2019); however, the mechanism by which NAM alters adaptive T cell immunity is unknown but is crucial to understand because this is a widely used human supplement. For example, it is unclear if NAM specifically affects naive T cell transition into effector T cells, effector function itself, or subsequent responses. To test this, purified naive splenic and lymph node T cells were differentiated into effectors using α-CD3/CD28 beads + rhIL-2 for 66 h and NAM impact on $CD8^+$ and $CD4^+$ T cell cytokine production was assessed. Compared to controls, $CD8^+$ T cells differentiated with α-CD3/CD28 beads + rhIL-2 in the presence of NAM released significantly lower amounts of cytokines associated with a cytokine storm, such as IFNγ, IL-2, IL-5, IL-10, IL-17A, but not IL-6 (Figure 1A). Similarly, naive $CD4^+$ T cells differentiated with α-CD3/CD28 beads + rhIL-2 in the presence of NAM released significantly less IFNγ, IL-5, IL-6, IL-10, IL-17A, but not IL-2 (Figure 1B). Importantly, this reduction in cytokine release was not because of an increased cell death (Figures 1C and 1D) or proliferation (Figure S1A). NAM was also able to significantly reduce IFNγ expression in both $CD8^+$ and $CD4^+$ T cells at both RNA and protein levels (Figures S1B and S1C). Thus, NAM limits $CD8^+$ and $CD4^+$ T cell differentiation to effectors and effector potential.

### NAM potently impairs $CD8^+$ T cell effector function

Next, we tested if NAM could impact already-differentiated effector $CD8^+$ and $CD4^+$ T cells. Thus, previously differentiated $CD8^+$ T cells in the presence or absence of NAM were restimulated with α-CD3/CD28 beads or with the TCR bypassing mitogen PMAi for 6 h, with or without NAM (Figure 2A). Effector $CD8^+$ T cells differentiated without NAM and restimulated with α-CD3/CD28 beads in the presence of NAM, secreted significantly less IFNγ, IL-2, IL-5, and IL-6 compared to vehicles (Figure 2B, left panel). When the same effector $CD8^+$ T cells were restimulated with PMAi, NAM did not have a significant effect on cytokine production (Figure 2B, right panel). Effector $CD8^+$ T cells previously differentiated in the presence of NAM and restimulated with α-CD3/CD28 beads with NAM, produced significantly less IFNγ, IL-2, and IL-5 compared to cells differentiated in the presence of NAM and restimulated with α-CD3/CD28 beads without NAM (Figure 2C, left panel). Again, PMAi stimulation of cytokine release was not affected by NAM (Figure 2C, right panel). Of note, cells differentiated with NAM and restimulated without NAM (Figure 2C, left panel, white bar), upon restimulation, could no longer produce expected levels of cytokines compared to cells differentiated and restimulated without NAM (Figure 2B, left panel, white bar). Importantly, this shows that NAM can negatively affect future responses of effector $CD8^+$ T cells when it is present at the differentiation stage but not later. Finally, NAM had a weaker effect on $CD4^+$ T cells (Figures S2A and S2B, left panels), suggesting that effector $CD4^+$ T cells are more resistant to NAM. NAM did not alter PMAi-induced cytokine responses with the exception of increasing IFNγ and IL-2 during the restimulation in cells differentiated without NAM (Figures S2A and 2B, right panels). Thus, NAM significantly impairs the production of several inflammatory cytokines produced by effector $CD8^+$ T cells even when they were fully differentiated in the absence of NAM, which prompted us to study the mechanism of NAM-based IFNγ inhibition.

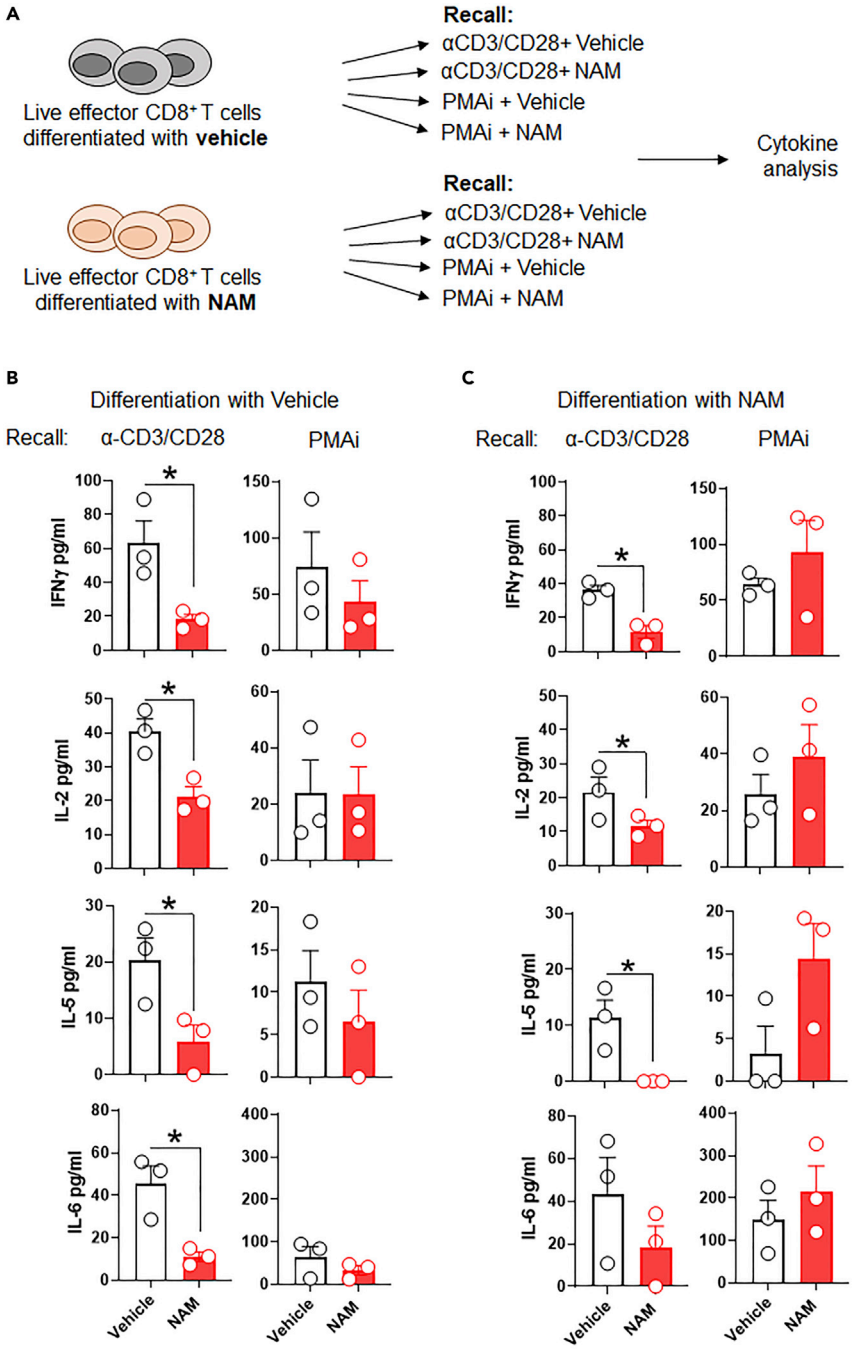


**Figure 2. NAM potently impairs CD8$^+$ T cell effector function**

(A) Schematic representation of live effector CD8$^+$ T cell restimulation.

(B) Cytokine secretion of CD8$^+$ T cells activated *in vitro* with α-CD3/CD28 beads plus rhIL-2 (30 U/mL) for 66 h, in the presence of vehicle and restimulated with either α-CD3/CD28 beads or PMAi for 6 h, with or without NAM.

(C) Cytokine secretion of CD8$^+$ T cells activated *in vitro* with α-CD3/CD28 beads plus rhIL-2 (30 U/mL) for 66 h, in the presence of NAM and restimulated with either α-CD3/CD28 beads or PMAi for 6 h, with or without NAM. Each dot represents an independent experiment (n = 3-4 mice/experiment). Data are represented as mean ± SEM. *p <0.05 by two-tailed unpaired t test. See also Figure S2.

## NAM regulates IFNγ secretion and cell metabolism in effector CD8$^+$ T cells

Given that NAM did not affect PMAi stimulation, it was reasoned that its mechanism of action may be TCR-dependent. Thus, the widely accepted TCR transgenic OT-I model of SIINFEKL peptide-specific CD8$^+$ T cells was used (Figure 3A). Specifically, OT-I CD8$^+$ T cells were adoptively transferred into recipient mice, then immunized the day after with SIINFEKL peptide plus the costimulatory agonists α-CD134/CD137 mAbs to induce the differentiation of CD8$^+$ effector T cells (Lee et al., 2004, 2007). These costimulatory pathways drive robust antitumor immunity, and have been associated with various inflammatory diseases such as atherosclerosis (Gotsman et al., 2008; Watts, 2005). To test the TCR-dependent postulate, day 4 SIINFEKL-primed and costimulated CD8$^+$ T cells were purified and restimulated *ex vivo* with SIINFEKL, PMAi, or three cytokine combinations of IL-2/IL-12 with members of the IL-1 family (IL-33 and IL-36β). These cytokine combinations provide a synergistic signal that induces robust IFNγ release in effector T cells, but in a TCR-independent manner (Morales Del Valle et al., 2019; Tsurutani et al., 2016). This "innate-like response" by T cells does not involve TCR activation, and should not be inhibited if NAM is dependent on TCR triggering. As expected, effector CD8$^+$ T cells restimulated with SIINFEKL released significantly less IFNγ when NAM was present in culture (Figures 3B and S3A), and this was not because of an increased apoptosis (Figure S3B). NAM did not affect stimulation by PMAi (Figure 3C), but surprisingly, when effector CD8$^+$ T cells were stimulated with cytokine combinations, NAM potently inhibited IFNγ release compared to vehicle (Figure 3D). Thus, NAM inhibits through TCR-dependent and independent pathways.

It is known that TCR dependent IFNγ production by activated CD8$^+$ T cells and the innate-like cytokine receptor IFNγ response are both directly coincident with glycolysis (Chang et al., 2013; Tsurutani et al., 2016). Thus, one reason for NAM-dependent IFNγ reduction could be from reduced glycolysis in effector CD8$^+$ T cells. However, effector CD8$^+$ T cells isolated 4 days after adoptive transfer and pretreated for 30 min with NAM, which then remained in the culture for a total of about 3 h, exhibited a significantly higher extracellular acidification rate (ECAR) relative to control cells, resulting in greater glycolytic power (Figure 3E). NAM is a precursor of NAD$^+$ (Mitchell et al., 2018; Rajman et al., 2018; Tan et al., 2019), the essential coenzyme involved in redox reactions during glycolysis. Thus, NAM could induce a glycolytic increase in CD8$^+$ T cells because of its conversion to NAD$^+$. Indeed, mass spectrometry analysis revealed that NAM addition resulted in a significant increase of extracellular NAD$^+$ (Figure 3F). To further confirm that NAD$^+$ alone is sufficient to increase glycolysis, exogenous NAD$^+$ was added to effector CD8$^+$ T cells for 30 min before ECAR was measured. As hypothesized, cells with NAD$^+$ exhibited a significantly higher ECAR compared to control cells (Figure 3G). Conversely, blockade of NAD$^+$ production from endogenous NAM with the nicotinamide phosphoribosyltransferase (NAMPT) inhibitor FK866, demonstrated that effector CD8$^+$ T cells stimulated with PMAi were no longer able to undergo glycolysis (Figure 3H) compared to vehicle. Altogether, these data indicate that NAM significantly enhances effector CD8$^+$ T cell glycolytic power because of its conversion to NAD$^+$, which surprisingly is inversely correlated to IFNγ release.

## NAM downregulates the mTORC1 pathway

A number of studies have shown that NAM inhibits SIRT1 (Bitterman et al., 2002; Mitchell et al., 2018), a deacetylase that induces deacetylation of inflammation-related transcription genes (Hwang et al., 2013; Liu and McCall, 2013). However, NAM can be reconverted to NAD$^+$, which is a SIRT1 activator (Hwang and Song, 2017). Furthermore, recent work have shed light on other molecular pathways possibly targeted by NAM (Daniel et al., 2007; Meng et al., 2018; Mouchiroud et al., 2013; Van Gool et al., 2009; Zhang et al., 2021). However, the mechanism by which NAM reduces cytokine production in T cells is unknown. First, we tested for any SIRT1 involvement in the NAM mechanism of action in CD8$^+$ T cells. Specifically, inhibiting SIRT1 activity using the SIRT1 inhibitor EX-527 did not affect IFNγ production in effector CD8$^+$ T cells, even in the presence of NAM (Figure S4A), which is expected to block the effect of EX-527 by increasing SIRT1 activity (Hwang and Song, 2017; Jang et al., 2012; Song et al., 2021). This result suggests that the mechanism by which NAM affects IFNγ in CD8 T cells is not necessarily through the activation of SIRT1. Given that NAM significantly reduces IFNγ release in effector CD8$^+$ T cells after SIINFEKL restimulation or via the innate-like cytokine receptor response, we reasoned that NAM should affect a pathway that is common between these two immune stimuli. The mechanistic target of rapamycin (mTOR) is a serine/threonine kinase that is part of two protein complexes mTORC1 and mTORC2. Although mTORC1 is more involved in protein (including cytokine), lipid, and nucleotide synthesis, mTORC2 plays a main role in survival and proliferation (Saxton and Sabatini, 2017), which are all key steps for T cell function. After restimulation with SIINFEKL, NAM significantly increased AMPK activity, a mTOR inhibitor, resulting in a reduction of phospho

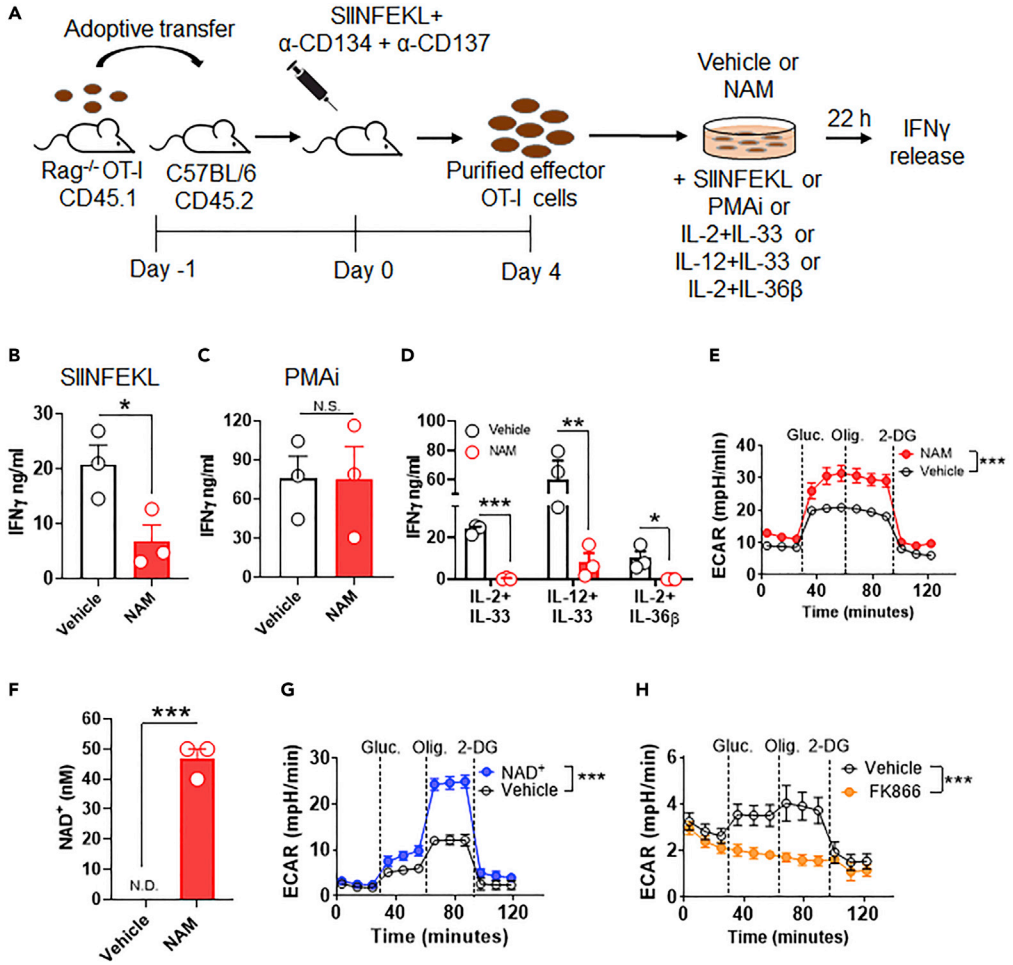


**Figure 3. NAM regulates IFNγ secretion and cell metabolism in effector CD8$^+$ T cells**

(A) Adoptive transfer of CD45.1$^+$ OT-I cells into CD45.2$^+$ C57BL/6J mice on day −1. On day 0 C57BL/6 CD45.2 are immunized with a specific peptide (SIINFEKL, 50 μg/mouse) plus αCD134/CD137 and to activate specific OT-I T cells. OT-I T cells are purified on day 4, cultured with or without NAM and restimulated for 22 h with SIINFEKL, IL-2+IL-33, IL-12+IL-33, IL-2+IL-36β, or PMAi and then ELISA on supernatants was performed to measure IFNγ secretion.

(B) IFNγ secretion of effector CD8$^+$ OT-I restimulated *ex vivo* with SIINFEKL (500 pg/mL) for 22 h in the presence of vehicle or NAM (10 mM). Two additional sources of NAM were used showing similar results (See Figure S3A).

(C) IFNγ secretion of effector OT-I cells restimulated *ex vivo* with PMAi for 22 h in the presence of vehicle or NAM (10 mM).

(D) IFNγ secretion of effector OT-I cells restimulated *ex vivo* with IL-2+IL-33, IL-12+IL-33, or IL-2+IL-36β for 22 h in the presence of vehicle or NAM (10 mM).

(E) ECAR of effector OT-I cells pre-incubated and cultured during the assay with either vehicle or NAM (10 mM). A representative of three independent experiments is shown. (F) Mass spectrometry analysis showing NAD$^+$ extracellular content from effector OT-I cells restimulated *ex vivo* with SIINFEKL (500 pg/mL) for 3 h in the presence of vehicle or NAM (10 mM).

(G) ECAR of effector OT-I cells preincubated and cultured during the assay with either vehicle or NAD$^+$ (1 mM). A representative of three independent experiments is shown.

(H) ECAR of effector OT-I cells restimulated *ex vivo* with PMAi, preincubated, and cultured during the assay with either vehicle or FK866 (30 nM). A representative of three independent experiments is shown. Each dot represents an independent experiment (n = 3-4 mice/experiment). Data are represented as mean ± SEM for combined plots and ± SD for representative plots. *p <0.05, **p <0.01, ***p <0.001, N.S. not significant by two-tailed unpaired t test (B–D and F) or area under the curve test (E, G, and H). N.D. not detected. See also Figure S3.

mTOR (Figures 4A and 4B). Without restimulation NAM had no apparent impact on the AMPK-mTOR axis (Figures 4A, 4B, and Table S2). Next, the downstream mTORC1 target S6 was examined, and consistent with the reduction of p-mTOR, the percentage of p-S6$^{hi}$ CD8$^+$ T cells was significantly lower when cells

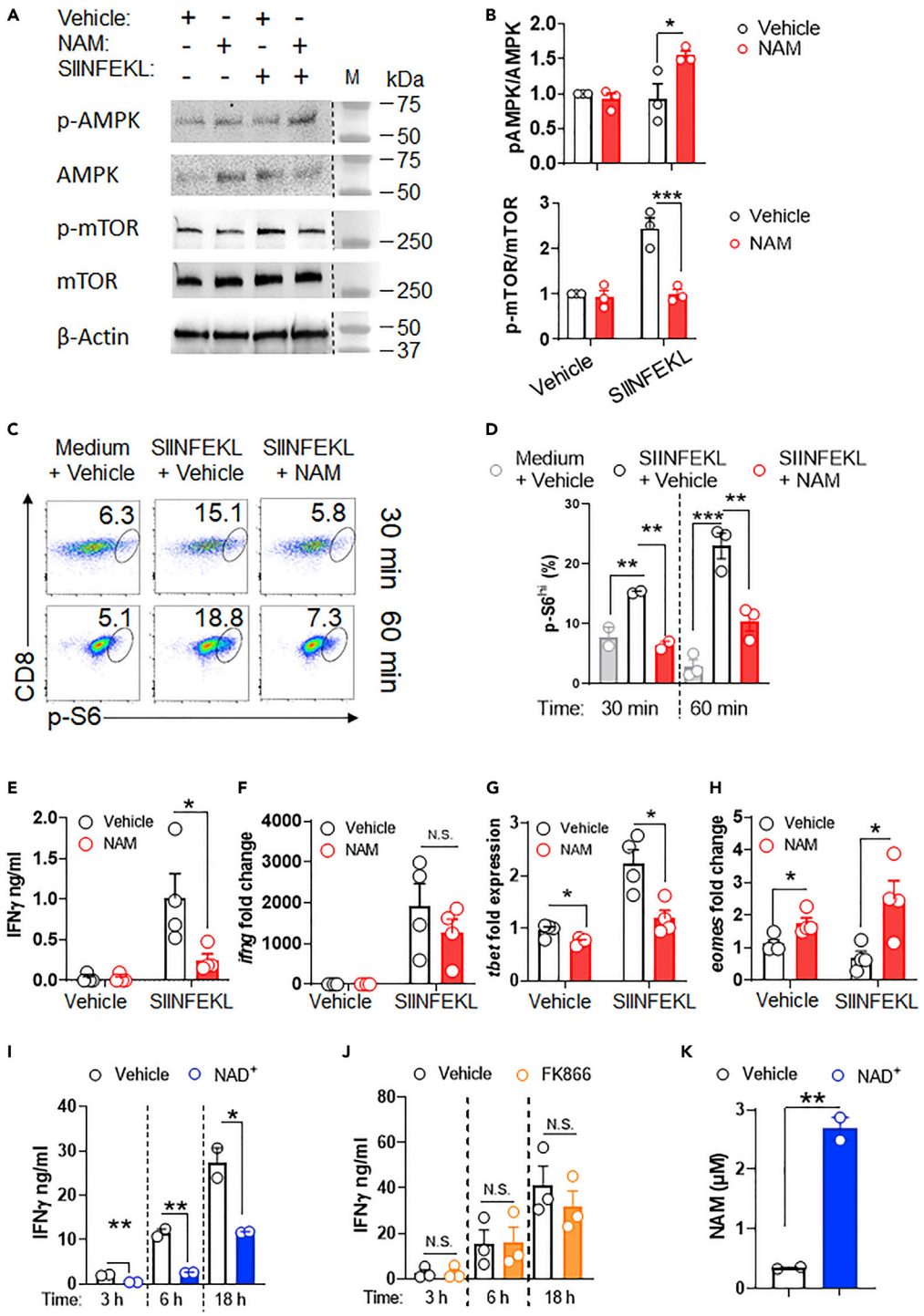


**Figure 4. NAM downregulates the mTORC1 pathway independently of NAD+**

(A) Western blot of the mTORC1 pathway in cytoplasmic lysates of effector OT-I cells restimulated *ex vivo* with medium or SIINFEKL (500 pg/mL), in the presence of vehicle or NAM (10 mM). Marker (M) position is on the right. A representative of three independent experiments is shown.

(B) Quantification of proteins shown in (A).

(C) p-S6 expression of effector OT-I cells without restimulation or restimulated *ex vivo* with SIINFEKL (500 pg/mL), in the presence of vehicle or NAM (10 mM) for 30 min and 60 min. A representative of at least two independent experiments is shown.

**Figure 4. *Continued***

(D) Percentage of the p-S6$^{hi}$ population showed in (C).

(E) IFNγ secretion of effector OT-I cells without restimulation or restimulated *ex vivo* with medium or SIINFEKL (500 pg/mL) for 3 h.

(F) *ifng* expression relative to β-actin of effector OT-I cells without restimulation or restimulated *ex vivo* with medium or SIINFEKL (500 pg/mL) for 3 h.

(G) *tbet* expression relative to β-actin of effector OT-I cells without restimulation or restimulated *ex vivo* with medium or SIINFEKL (500 pg/mL) for 3 h.

(H) *eomesodermin* expression relative to β-actin of effector OT-I cells without restimulation or restimulated *ex vivo* with medium or SIINFEKL (500 pg/mL) for 3 h.

(I) IFNγ secretion of effector OT-I cells restimulated *ex vivo* with SIINFEKL (500 pg/mL), with or without NAD$^+$ (1 mM) for 3, 6, and 18 h.

(J) IFNγ secretion of effector OT-I cells restimulated *ex vivo* with SIINFEKL (500 pg/mL), with or without FK866 (30 nM) for 3, 6, and 18 h.

(K) Mass spectrometry analysis showing NAM extracellular content from effector OT-I cells restimulated *ex vivo* with SIINFEKL (500 pg/mL) for 6 h in presence of vehicle or NAD$^+$ (1 mM). Each dot represents an independent experiment (n = 3-4 mice/experiment). Data are represented as the mean ± SEM. *p <0.05, **p <0.01, ***p <0.001. N.S. not significant by two-tailed unpaired t test (B and E-K) or one-way ANOVA test (D). See also Figure S4.

were restimulated with SIINFEKL or with cytokines in the presence of NAM (Figures 4C, 4D, and S4C). Of note, compared to controls, the increase of S6 phosphorylation (and thus of mTORC1 activity) in response to the TCR activation (Figures 4C and 4D) is much stronger compared to cytokines (Figure S4C). However, even that modest increase by the cytokines is shut down by NAM, bringing it to a lower level than control (gray bar). Again, the action of PMAi overpowered the inhibitory effect of NAM (Figure S4B), suggesting that PMAi is a too strong of an mTORC1 activator (around 70% of the cells are p-S6$^{hi}$ positive after PMAi restimulation versus 25% seen after SIINFEKL restimulation) which may override any effect induced by NAM. The mTORC1 pathway is involved in protein translation as one of its major functions (Ma and Blenis, 2009). To test if NAM acts by affecting the mTORC1 activity via protein translation, a 3 h post SIINFEKL re-stimulation was assessed for both release of IFNγ protein and for *ifng* transcription. Thus, effector CD8$^+$ T cells cultured in the presence of NAM exhibited a significant decrease of IFNγ release compared to vehicle (Figure 4E), whereas early *ifng* transcription remained unchanged (Figure 4F), unlike later time points (Figure S1B) which are likely a function of positive feedback by IFNg itself from the vehicle treated effectors. Thus, NAM inhibition of mTOR impairs *ifng* mRNA translation, not early gene transcription of IFNγ.

mTOR is vital to effector/memory CD8$^+$ T cell fate through the regulation of two key transcription factors, T-bet and Eomesodermin. Specifically, although effector CD8$^+$ T cells augment mTOR activity leading to *tbet* induction and decreasing *eomesodermin*, memory CD8$^+$ T cells show the opposite effect (Araki et al., 2009; Rao et al., 2010). To further confirm the NAM-dependent mTOR inhibition, effector CD8$^+$ T cells cultured in the presence of NAM, compared to vehicle, exhibited reduced *tbet* and increased *eomesoderim* (Figures 4G and 4H). Consistently, NAM also significantly increased the percentage of CD44$^+$ CD62L$^+$ CD4$^+$ and CD8$^+$ T cells (memory phenotype) compared to vehicle, without changing the percentage of effector cells (CD44$^+$ CD62L$^-$) (Figure S4D). Thus, NAM might be used to promote memory T cell differentiation.

Next, we tested if the inhibitory effect of NAM on mTORC1 was because of its conversion to NAD$^+$. Without restimulation, the percentage of the p-S6$^{hi}$ population was even higher in the presence of NAD$^+$. Conversely, when effector CD8$^+$ T cells were restimulated with SIINFEKL for 30 min, the p-S6$^{hi}$ population in the presence of NAD$^+$ was comparable to vehicles. This percentage started to decrease after 60 min (Figure S4E), suggesting that NAD$^+$ can negatively affect S6 phosphorylation only with a longer incubation. Consistently, the addition of NAD$^+$ during restimulation of effector CD8$^+$ T cells significantly reduced IFNγ release after 3 h and continued through a time course (Figure 4I). However, when NAD$^+$ production from endogenous NAM was inhibited by FK866, the IFNγ release was not affected (Figure 4J), despite FK866 ability to block glycolysis (Figure 3H), suggesting that NAD$^+$ is not directly involved in the IFNγ release in CD8$^+$ T cells. Of note, adding exogenous NAM in the presence of FK866 blockade is not feasible because high concentrations of NAM are an antidote for FK866 action and would reverse inhibition (Hasmann and Schemainda, 2003). These results indicate that NAD$^+$ does not inhibit the mTORC1 pathway directly; rather, its effect at later time points is likely because of the conversion of NAD$^+$ into NAM (Rajman et al., 2018). This hypothesis was indeed confirmed because exogenous NAD$^+$ resulted in a significantly

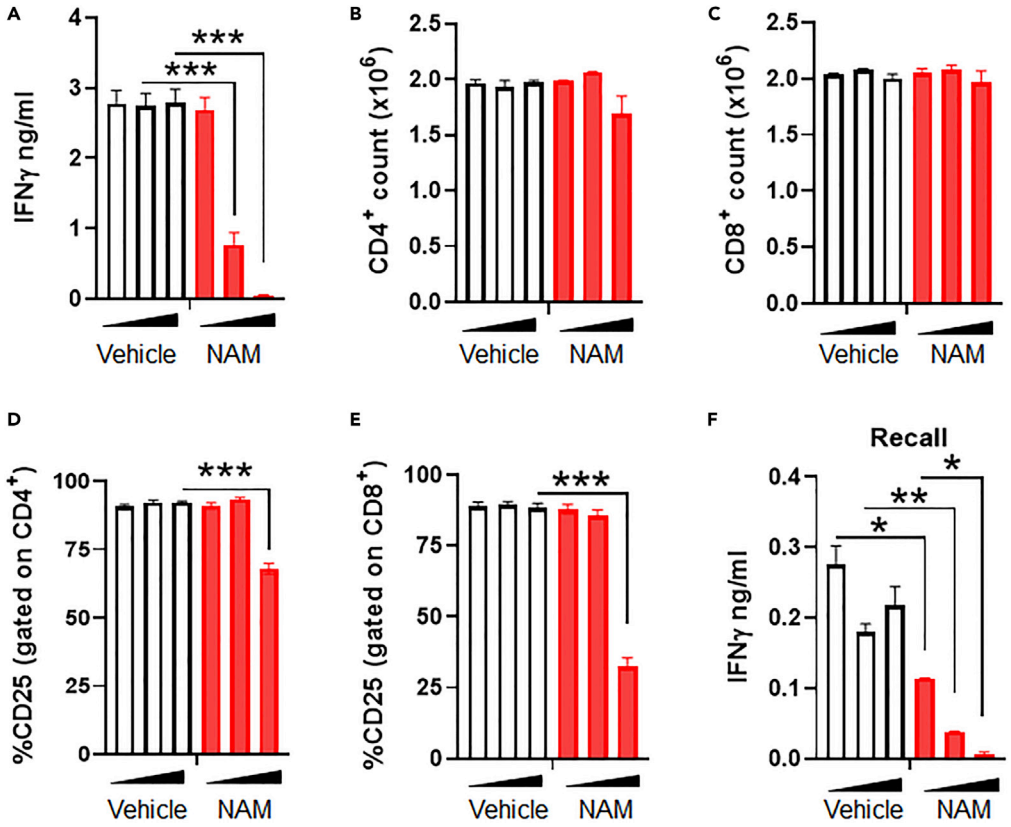


**Figure 5. NAM blocks human effector T cell potential and function**

(A) IFNγ secretion of human PBMCs activated *in vitro* with α-CD3/CD28 beads (1:1 ratio) for 4 days in the presence of vehicle or NAM (3, 10, and 30 mM).

(B) Count of live $CD4^+$ T cells in human PBMCs activated *in vitro* with α-CD3/CD28 beads (1:1 ratio) for 4 days in the presence of vehicle or NAM (3, 10, and 30 mM). Numbers are given by multiplying total cell number by live cell percentage after live/dead staining.

(C) Count of live $CD8^+$ T cells in human PBMCs activated *in vitro* with α-CD3/CD28 beads (1:1 ratio) for 4 days in the presence of vehicle or NAM (3, 10, and 30 mM). Numbers are given by multiplying total cell number by live cell percentage after live/dead staining.

(D) Percentage of CD25 expression on live $CD4^+$ T cells in human PBMCs activated *in vitro* with α-CD3/CD28 beads (1:1 ratio) for 4 days in the presence of vehicle or NAM (3, 10, and 30 mM).

(E) Percentage of CD25 expression on live $CD8^+$ T cells in human PBMCs activated *in vitro* with α-CD3/CD28 beads (1:1 ratio) for 4 days in the presence of vehicle or NAM (3, 10, and 30 mM).

(F) IFNγ secretion of human PBMCs activated *in vitro* with α-CD3/CD28 beads (1:1 ratio) for 4 days and restimulated in the presence of vehicle or NAM (3, 10, and 30 mM) for 6 h. (A)–(C) are represented as the mean ± SEM of two independent experiments. (D) – (F) are representatives of two independent experiments showing the same results. *p <0.05, **p <0.01, ***p <0.001 by two-tailed unpaired t test. See also Figure S5.

increased extracellular NAM content (Figure 4K). To study whether NAM could affect the mTORC2 pathway we looked at one of its downstream molecules, NF-κB (Lee et al., 2010). With or without SIINFEKL restimulation, NF-κB nuclear translocation was not affected by NAM (Figure S4F). All these results indicate that supplemental NAM acts specifically by inhibiting the mTORC1 pathway, resulting in a significant decrease of IFNγ mRNA translation. This effect is intrinsically NAM-dependent and is not because of NAM conversion to $NAD^+$.

## NAM blocks human effector T cell potential and function

To dissect the role of exogenous NAM in human T cells, PBMCs samples from healthy donors were used and T cells were activated using α-CD3/CD28 beads for 6 days in the presence of three different doses of NAM. As shown in Figure 5A, NAM significantly reduced IFNγ secretion by T cells in a dose-dependent manner without affecting cell viability of $CD4^+$ (Figure 5B) and $CD8^+$ T cells (Figure 5C). Of note, at the

highest dose of NAM, both $CD4^+$ and $CD8^+$ T cells significantly reduced CD25 expression compared to control cells (Figures 5D and 5E), suggesting impaired IL-2 responsiveness. Consistent with the data from mouse cells, human effector T cells restimulated in the presence of NAM, secreted significantly less IFNγ compared to the vehicle (Figure 5F). Finally, we enhanced stimulation strength by doubling the bead to cell ratio. Although the middle dose of NAM was now ineffective, the highest dose was still able to decrease IFNγ production (Figure S5A). Upon restimulation, all the doses significantly reduced IFNγ release compared to vehicles (Figure S5B). These data show that NAM blocks human T cell effector function and is potentially translatable to controlling human adaptive immune responses.

### NAM inhibits T cell responses *in vivo*

In recent years, the role of NAM *in vivo* has been controversial. Two studies demonstrated that NAM mediates chemopreventive effects by boosting immune cell cytokine production in different models of murine cancers (Buque et al., 2020; Scatozza et al., 2020). Conversely, other studies showed that NAM supplementation reduced inflammation protecting against high fat diet-induced inflammation (Mendez-Lara et al., 2021; Mitchell et al., 2018), an Experimental Autoimmune Encephalitis (EAE) model (Kaneko et al., 2006), and pulmonary injury caused by ischemia/reperfusion in rats (Su et al., 2007).

To dissect the precise role of NAM during *in vivo* T cell responses we took advantage of *S. aureus* enterotoxin A, an immunogen that directly activates specific TCR Vβ chains (e.g., Vβ3) but not Vβ14 (Herman et al., 1991). When delivered intranasally, this model induces acute lung injury (Kumar et al., 2010; Menoret et al., 2018; Svedova et al., 2017), leading to life threatening complications including diffuse alveolar damage (DAD), acute lung injury (ALI), and acute respiratory distress syndrome (ARDS). Secondly, this response greatly impacts $CD8^+$ T cells and IFNγ (Muralimohan et al., 2008) which we have shown are targets for NAM. To recapitulate a typical human scenario, mice were fed a standard diet or one supplemented with NAM for 2 weeks and then intranasally challenged with *S. aureus* enterotoxin A. During the course of the study, NAM did not alter body weight nor food consumption (Figures 6A and 6B). However, 6 h post *S. aureus* enterotoxin A inhalation the NAM-fed mice exhibited an increased content of serum NAM (Figure 6C), coupled with a significant decrease of serum IL-2 compared to control mice (Figure 6D). Importantly, the total number and the percentage of *S. aureus* enterotoxin A responding (TCR Vβ3) $CD8^+$ and $CD4^+$ T cells were significantly reduced in peripheral lymph nodes of mice that received the NAM diet (Figures 6E, 6F, and S6A). In contrast, the number and the percentage of non-*S. aureus* enterotoxin A-responding (TCR Vβ14) $CD8^+$ and $CD4^+$ T cells were unaffected in the presence of NAM diet (Figures S6B and S6C). Lastly, when cells from peripheral lymph nodes of mice fed with the NAM diet were restimulated *in vitro*, the number of IFNγ-producing $CD8^+$ T cells was significantly reduced compared to control mice, and this included a modest decrease in mean intensity fluorescence (Figures 6G and 6H). Altogether, our results show that NAM inhibits T cell clonal expansion and effector cytokine production *in vivo*, and may inhibit over activation of T cell responses.

## DISCUSSION

In the last decade, the role of metabolic pathways in the regulation of immune responses has emerged, bringing to the rise of a new field called immunometabolism (Makowski et al., 2020; O'Neill et al., 2016; Patel et al., 2019). Moreover, several studies have shown how specific metabolites are able to regulate T cell function and fate (Okano et al., 2017; Qiu et al., 2019; Tyrakis et al., 2016). NAM is an immunometabolite known to exert beneficial effects in a variety of biological events, such as aging, oxidative stress and inflammation (Mitchell et al., 2018; Mouchiroud et al., 2013; Tran et al., 2016). However, the role of NAM on adaptive immune responses has been insufficiently investigated, despite the many reports of its immune altering power. One of the paradigms of immunometabolism is that effector T cells are highly glycolytic and glycolysis is required for effector cytokine production in T cells (Chang et al., 2013; O'Neill et al., 2016). In this study, we demonstrated that although NAM increases the glycolytic potential of effector $CD8^+$ T cells (Figure 3E), it strongly impairs $CD8^+$ T cell differentiation and effector function (Figures 1, 2, and 3B) via mTORC1 (Figures 4A–4H) and independently of $NAD^+$ (Figures 4I–4K). To the best of our knowledge, this is the first report of a metabolic compound able to boost T cell glycolysis, yet leading to a decrease in T cell effector function. Of note, NAM exerts a potential translatable effect also on human adaptive immunity. In fact, NAM inhibits IFNγ and CD25 expression in activated human T cells (Figure 5). Although NAM could affect CD25 expression by inducing CD25 ADP-ribosylation in Tregs (Teege et al., 2015), activated T cells have been shown to be resistant to ADP-ribosylation of surface protein (Kahl et al., 2000), leaving the question on how NAM affects CD25 expression in T cells still open.

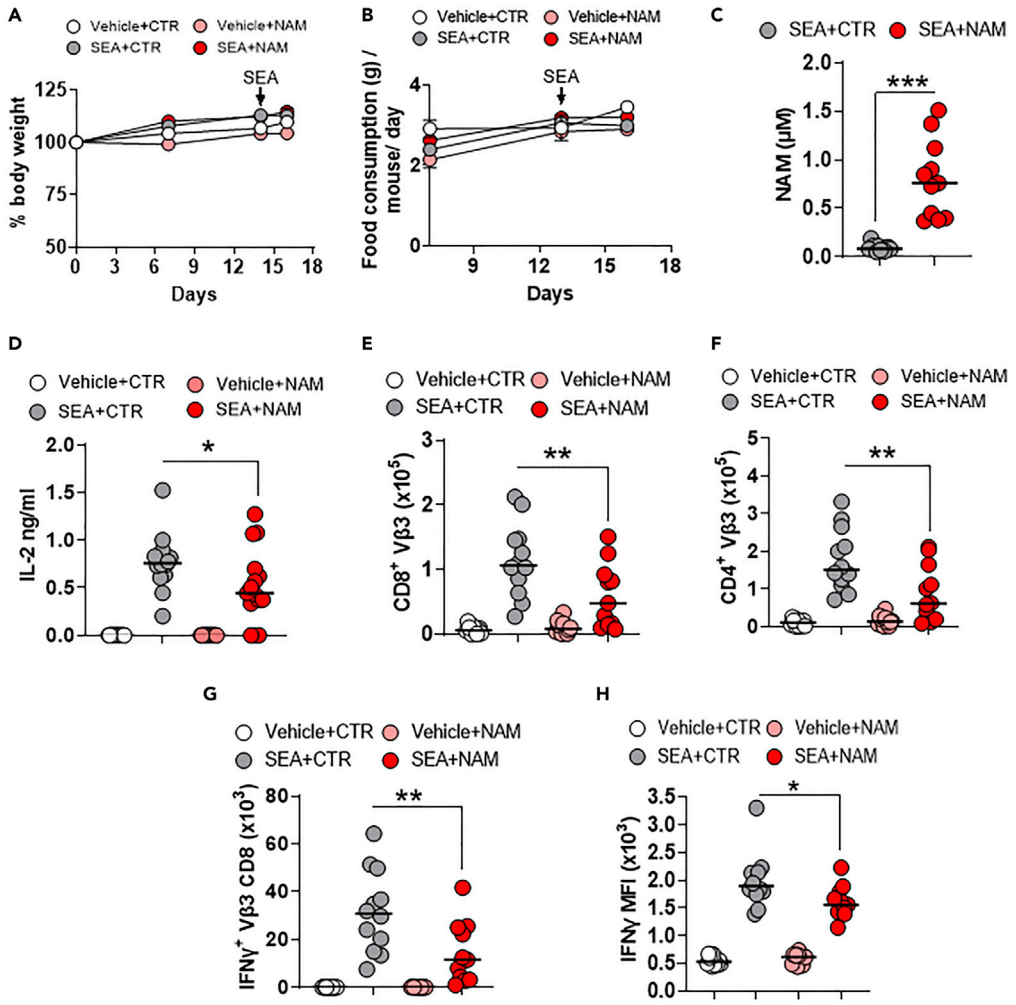


**Figure 6. NAM inhibits T cell response *in vivo***

(A) Body weight percentage of mice fed a control diet or a NAM-supplemented diet (125 mg/kg/day) before and after SEA immunization (1 μg/mouse). A representative of four independent experiments is shown.

(B) Daily food consumption of mice fed a control diet or a NAM-supplemented diet (125 mg/kg/day) before and after SEA immunization (1 μg/mouse). A representative of four independent experiments is shown.

(C) Mass spectrometry analysis showing NAM concentration in the serum of mice fed a control diet or a NAM-supplemented diet (125 mg/kg/day) 6 h post SEA immunization (1 μg/mouse).

(D) Serum IL-2 in mice fed a control diet or a NAM-supplemented diet (125 mg/kg/day) 6 h post SEA immunization (1 μg/mouse).

(E) Number of Vβ3 $CD8^+$ T cells in peripheral LNs of mice fed a control diet or a NAM-supplemented diet (125 mg/kg/day) 48 h post SEA immunization (1 μg/mouse).

(F) Number of Vβ3 $CD4^+$ T cells in peripheral LNs of mice fed a control diet or a NAM-supplemented diet (125 mg/kg/day) 48 h post SEA immunization (1 μg/mouse).

(G) Number of IFNγ-producing Vβ3 $CD8^+$ T cells in peripheral LNs of mice fed with control diet or NAM-supplemented diet (125 mg/kg/day) 48 h post SEA immunization (1 μg/mouse).

(H) MFI of IFNγ-producing Vβ3 $CD8^+$ T cells in peripheral LNs of mice fed a control diet or a NAM-supplemented diet (125 mg/kg/day) 48 h post SEA immunization (1 μg/mouse). Each dot represents an individual mouse (n = 4 mice per group). (A) and (B) are representative of four independent experiments showing similar results. (C)–(H) are represented as the mean ± SEM of at least three independent experiments.*p <0.05, **p <0.01, N.S. not significant by one-way ANOVA test. See also Figure S6.

To date, the impact of NAM on *in vivo* immune responses has been varied. NAM was shown to reduce neutrophil and $CD4^+$ T cell infiltration during *C. rodentium*-induced colitis and in an Experimental Autoimmune Encephalitis (EAE) model, respectively (Bettenworth et al., 2014; Kaneko et al., 2006).

Conversely, other studies demonstrated that NAM mediates chemopreventive effects by boosting T cell response and cytokine production in different models of murine cancers (Buque et al., 2020; Scatozza et al., 2020) and mediates *S. aureus* clearance in a neutrophil-dependent fashion (Kyme et al., 2012). Thus, it is likely that the effect of NAM on immune cells can be either inhibitory or stimulatory depending on several factors, such as dose, administration route, and cellular context. Presently, million people are taking NAM dietary supplements to extend life span and prevent aging and inflammation; however, there are still unanswered questions on the function of NAM on immunity. As an example: will NAM supplementation be more valuable before vaccination, or instead will it be more effective in preventing tissue damage such as lung injury? When is the right time to start NAM supplementation? More studies are necessary to avoid unexpected or unwanted outcomes.

Several mechanisms of action have been proposed for NAM in different cell types, suggesting the complexity of its action. NAM was shown to be a SIRT1 inhibitor, facilitating the expansion of hematopoietic progenitors, restoring cognition in Alzheimer's diseases, and ameliorating mouse health span (Green et al., 2008; Mitchell et al., 2018; Peled et al., 2012). On the contrary, NAM was reported to increase mitophagy because of $NAD^+$ content increase and subsequent SIRT1 and AMPK activation in human fibroblasts (Jang et al., 2012; Song et al., 2021). In mouse hepatocytes, NAM-dependent increase of $NAD^+$ induces the activation of the antioxidant gene FOXO, improving metabolic health, and extending life span (Mouchiroud et al., 2013). In addition, NAM plays an inhibitory role on ROCK/CK1 kinases in human pluripotent stem cells (Meng et al., 2018), on ERK phosphorylation in B cells (Daniel et al., 2007), on SIRT6 activity in macrophages and dendritic cells (Van Gool et al., 2009), and on MAPK and NF-κB activity in macrophages (Zhang et al., 2021). In this study, we show that the molecular mechanism by which NAM reduces IFNγ in $CD8^+$ effector T cells is dependent on the mTORC1 pathway through AMPK activation (Figures 4A–4D). It is well known that AMPK activation can be triggered by an increase of AMP/ADP ratio or a $Ca^{2+}$ increase (Shackelford and Shaw, 2009). Here we show that SIRT1 is not involved in the NAM-dependent IFNγ decrease in CD8 T cells; thus, it is possible that in these cells AMPK is activated by other mechanisms. However, more studies are needed to better understand the molecular mechanism by which NAM induces AMPK activation in $CD8^+$ T cells. Consistent with mTORC1 involvement in protein synthesis (Saxton and Sabatini, 2017), NAM-dependent mTORC1 inhibition leads to a significant decrease of IFNγ translation in effector $CD8^+$ T cells (Figures 4E and 4F). However, NAM eventually affects IFNγ transcription at later time points (Figure S1C), which is probably because of an IFNγ-driven feedback loop. mTOR determines T cell effector/memory fate through transcriptional regulation of *tbet* and *eomesodermin* (Araki et al., 2009; Rao et al., 2010). We found that NAM-associated mTOR inhibition reduces *tbet* and enhances *eomesodermin* transcription (Figures 4G and 4H), suggesting a potential use of NAM in generating memory T cells. Furthermore, our work shows that the inhibitory effect of NAM on mTORC1 is not dependent on $NAD^+$ (Figures 4I–4K), pointing out the intrinsic biological relevance of NAM, which therefore does not act only as a $NAD^+$ booster (Rajman et al., 2018).

*S. aureus* enterotoxin A is a superantigen that activates specific TCR Vβ T cells (Herman et al., 1991) and induces acute lung injury (Kumar et al., 2010; Li et al., 2020; Menoret et al., 2018; Svedova et al., 2017), exerting a major effect on $CD8^+$ T cells infiltration and IFNγ production (Muralimohan et al., 2008). Other studies have addressed the effect of NAM in innate immune and inflammatory responses against acute lung injury (Su et al., 2007; Zhang et al., 2021). However, the role of NAM on the adaptive arm is completely unknown. In this study, we have used *S. aureus* enterotoxin A as a model of direct T cell response *in vivo*. A NAM supplementation reduces *S. aureus* enterotoxin A-specific $CD4^+$ and $CD8^+$ T cell expansion and serum IL-2 *in vivo*, and decreases the ability of effector $CD8^+$ T cell population to produce IFNγ in response to a second stimulation with *S. aureus* enterotoxin A (Figures 6 and S6). Overall, our study reveals an inhibitory effect of NAM on $CD8^+$ T cell differentiation and effector function. Thus, NAM supplementation could potentially prevent the development of diseases associated with T cell hyperactivation, and ameliorate the prognosis in hospitalized patients. Importantly, NAM would not wipe out the entire $CD8^+$ T cell response which is needed to restrain the virus outside of the lung and also to fight coinfections.

## Limitations of the study

This study presents some limitations. Firstly, like other studies, we used a high NAM concentration for the cell culture experiments, and therefore the biological significance should be carefully interpreted. Secondly, although we demonstrated that in $CD8^+$ T cells NAM regulates IFNγ release presumably through the AMPK/mTOR axis, how NAM activates AMPK needs further investigation. Lastly, this work has shown

that NAM induces the expression of memory markers in T cells; however, more studies should be performed to better dissect the role of NAM on memory T cell differentiation and function *in vivo*.

## STAR★METHODS

Detailed methods are provided in the online version of this paper and include the following:

- KEY RESOURCES TABLE
- RESOURCE AVAILABILITY
  - Lead contact
  - Materials availability
  - Data and code availability
- EXPERIMENTAL MODEL AND SUBJECT DETAILS
  - Mice and adoptive transfer
  - *In vitro* and *ex vivo* cell culture
  - Human cells
- METHODS DETAILS
  - *S. aureus* enterotoxin A immunization and diet
  - Flow cytometry
  - Quantitative real-time RT-PCR
  - Cytokine secretion analysis
  - Immunoblotting
  - Glycolysis assay
  - NAM and $NAD^+$ metabolite measurement
- QUANTIFICATION AND STATISTICAL ANALYSIS

## SUPPLEMENTAL INFORMATION

Supplemental information can be found online at https://doi.org/10.1016/j.isci.2022.103932.

## ACKNOWLEDGMENTS

We are thankful to Drs. Rachel Page and Vijay Rathinam for their critical reading of the manuscript and valuable feedback. This work was supported in part by NIH grants P01AI056172 and R21AI139891, institutional support, and Boehringer Ingelheim endowed Chair in Immunology.

## AUTHOR CONTRIBUTION

A.T.V. and F.A. conceived and designed the experiments. F.A., T.A.K., and A.M. performed the experiments and data analysis. A.P. performed the UHPLC-QTOF HRMS analysis. F.A. drafted the manuscript. A.M. and T.A.K. reviewed the manuscript. A.T.V. supervised the study and finalized the manuscript. All authors read and approved the final manuscript.

## DECLARATION OF INTERESTS

The authors declare no competing financial interests.

Received: October 27, 2021
Revised: January 14, 2022
Accepted: February 10, 2022
Published: March 18, 2022

## REFERENCES

Araki, K., Turner, A.P., Shaffer, V.O., Gangappa, S., Keller, S.A., Bachmann, M.F., Larsen, C.P., and Ahmed, R. (2009). mTOR regulates memory CD8 T-cell differentiation. Nature *460*, 108–112.

Bettenworth, D., Nowacki, T.M., Ross, M., Kyme, P., Schwammbach, D., Kerstiens, L., Thoennissen, G.B., Bokemeyer, C., Hengst, K., Berdel, W.E., et al. (2014). Nicotinamide treatment ameliorates the course of experimental colitis mediated by enhanced neutrophil-specific antibacterial clearance. Mol. Nutr. Food Res. *58*, 1474–1490.

Bitterman, K.J., Anderson, R.M., Cohen, H.Y., Latorre-Esteves, M., and Sinclair, D.A. (2002). Inhibition of silencing and accelerated aging by nicotinamide, a putative negative regulator of yeast sir2 and human SIRT1. J. Biol. Chem. *277*, 45099–45107.

Blacher, E., Bashiardes, S., Shapiro, H., Rothschild, D., Mor, U., Dori-Bachash, M., Kleimeyer, C., Moresi, C., Harnik, Y., Zur, M., et al. (2019). Potential roles of gut microbiome and metabolites in modulating ALS in mice. Nature *572*, 474–480.

Bogan, K.L., and Brenner, C. (2008). Nicotinic acid, nicotinamide, and nicotinamide riboside: a molecular evaluation of NAD+ precursor vitamins in human nutrition. Annu. Rev. Nutr. *28*, 115–130.

Buque, A., Bloy, N., Kroemer, G., and Galluzzi, L. (2021). Possible mechanisms of cancer prevention by nicotinamide. Br. J. Pharmacol. *178*, 2034–2040.

Buque, A., Bloy, N., Perez-Lanzon, M., Iribarren, K., Humeau, J., Pol, J.G., Levesque, S., Mondragon, L., Yamazaki, T., Sato, A., et al. (2020). Immunoprophylactic and immunotherapeutic control of hormone receptor-positive breast cancer. Nat. Commun. *11*, 3819.

Chang, C.H., Curtis, J.D., Maggi, L.B., Jr., Faubert, B., Villarino, A.V., O'Sullivan, D., Huang, S.C., van der Windt, G.J., Blagih, J., Qiu, J., et al. (2013). Posttranscriptional control of T cell effector function by aerobic glycolysis. Cell *153*, 1239–1251.

Chen, A.C., Martin, A.J., Choy, B., Fernandez-Penas, P., Dalziell, R.A., McKenzie, C.A., Scolyer, R.A., Dhillon, H.M., Vardy, J.L., Kricker, A., et al. (2015). A phase 3 randomized trial of nicotinamide for skin-cancer chemoprevention. N. Engl. J. Med. *373*, 1618–1626.

Daniel, J., Marechal, Y., Van Gool, F., Andris, F., and Leo, O. (2007). Nicotinamide inhibits B lymphocyte activation by disrupting MAPK signal transduction. Biochem. Pharmacol. *73*, 831–842.

Falconer, J., Pucino, V., Clayton, S.A., Marshall, J.L., Raizada, S., Adams, H., Philp, A., Clark, A.R., Filer, A., Raza, K., et al. (2021). Spontaneously resolving joint inflammation is characterised by metabolic agility of fibroblast-like synoviocytes. Front. Immunol. *12*, 725641.

Gotsman, I., Sharpe, A.H., and Lichtman, A.H. (2008). T-cell costimulation and coinhibition in atherosclerosis. Circ. Res. *103*, 1220–1231.

Green, K.N., Steffan, J.S., Martinez-Coria, H., Sun, X., Schreiber, S.S., Thompson, L.M., and LaFerla, F.M. (2008). Nicotinamide restores cognition in Alzheimer's disease transgenic mice via a mechanism involving sirtuin inhibition and selective reduction of Thr231-phosphotau. J. Neurosci. *28*, 11500–11510.

Hara, N., Yamada, K., Shibata, T., Osago, H., Hashimoto, T., and Tsuchiya, M. (2007). Elevation of cellular NAD levels by nicotinic acid and involvement of nicotinic acid phosphoribosyltransferase in human cells. J. Biol. Chem. *282*, 24574–24582.

Hasmann, M., and Schemainda, I. (2003). FK866, a highly specific noncompetitive inhibitor of nicotinamide phosphoribosyltransferase, represents a novel mechanism for induction of tumor cell apoptosis. Cancer Res. *63*, 7436–7442.

Herman, A., Kappler, J.W., Marrack, P., and Pullen, A.M. (1991). Superantigens: mechanism of T-cell stimulation and role in immune responses. Annu. Rev. Immunol. *9*, 745–772.

Hwang, E.S., and Song, S.B. (2017). Nicotinamide is an inhibitor of SIRT1 in vitro, but can be a stimulator in cells. Cell Mol Life Sci *74*, 3347–3362.

Hwang, J.W., Yao, H., Caito, S., Sundar, I.K., and Rahman, I. (2013). Redox regulation of SIRT1 in inflammation and cellular senescence. Free Radic. Biol. Med. *61*, 95–110.

Jang, S.Y., Kang, H.T., and Hwang, E.S. (2012). Nicotinamide-induced mitophagy: event mediated by high NAD+/NADH ratio and SIRT1 protein activation. J. Biol. Chem. *287*, 19304–19314.

Kahl, S., Nissen, M., Girisch, R., Duffy, T., Leiter, E.H., Haag, F., and Koch-Nolte, F. (2000). Metalloprotease-mediated shedding of enzymatically active mouse ecto-ADP-ribosyltransferase ART2.2 upon T cell activation. J. Immunol. *165*, 4463–4469.

Kaneko, S., Wang, J., Kaneko, M., Yiu, G., Hurrell, J.M., Chitnis, T., Khoury, S.J., and He, Z. (2006). Protecting axonal degeneration by increasing nicotinamide adenine dinucleotide levels in experimental autoimmune encephalomyelitis models. J. Neurosci. *26*, 9794–9804.

Kumar, S., Colpitts, S.L., Menoret, A., Budelsky, A.L., Lefrancois, L., and Vella, A.T. (2013). Rapid alphabeta T-cell responses orchestrate innate immunity in response to Staphylococcal enterotoxin A. Mucosal Immunol. *6*, 1006–1015.

Kumar, S., Menoret, A., Ngoi, S.M., and Vella, A.T. (2010). The systemic and pulmonary immune response to staphylococcal enterotoxins. Toxins (Basel) *2*, 1898–1912.

Kyme, P., Thoennissen, N.H., Tseng, C.W., Thoennissen, G.B., Wolf, A.J., Shimada, K., Krug, U.O., Lee, K., Muller-Tidow, C., Berdel, W.E., et al. (2012). C/EBPepsilon mediates nicotinamide-enhanced clearance of Staphylococcus aureus in mice. J. Clin. Invest. *122*, 3316–3329.

Lee, K., Gudapati, P., Dragovic, S., Spencer, C., Joyce, S., Killeen, N., Magnuson, M.A., and Boothby, M. (2010). Mammalian target of rapamycin protein complex 2 regulates differentiation of Th1 and Th2 cell subsets via distinct signaling pathways. Immunity *32*, 743–753.

Lee, S.J., Myers, L., Muralimohan, G., Dai, J., Qiao, Y., Li, Z., Mittler, R.S., and Vella, A.T. (2004). 4-1BB and OX40 dual costimulation synergistically stimulate primary specific CD8 T cells for robust effector function. J. Immunol. *173*, 3002–3012.

Lee, S.J., Rossi, R.J., Lee, S.K., Croft, M., Kwon, B.S., Mittler, R.S., and Vella, A.T. (2007). CD134 costimulation couples the CD137 pathway to induce production of supereffector CD8 T cells that become IL-7 dependent. J. Immunol. *179*, 2203–2214.

Li, L., Huang, Q., Wang, D.C., Ingbar, D.H., and Wang, X. (2020). Acute lung injury in patients with COVID-19 infection. Clin. Transl Med. *10*, 20–27.

Liu, T.F., and McCall, C.E. (2013). Deacetylation by SIRT1 reprograms inflammation and cancer. Genes Cancer *4*, 135–147.

Livak, K.J., and Schmittgen, T.D. (2001). Analysis of relative gene expression data using real-time quantitative PCR and the 2(-Delta Delta C(T)) Method. Methods *25*, 402–408.

Ma, X.M., and Blenis, J. (2009). Molecular mechanisms of mTOR-mediated translational control. Nat. Rev. Mol. Cell Biol. *10*, 307–318.

Makowski, L., Chaib, M., and Rathmell, J.C. (2020). Immunometabolism: from basic mechanisms to translation. Immunol. Rev. *295*, 5–14.

Mendez-Lara, K.A., Rodriguez-Millan, E., Sebastian, D., Blanco-Soto, R., Camacho, M., Nan, M.N., Diarte-Anazco, E.M.G., Mato, E., Lope-Piedrafita, S., Roglans, N., et al. (2021). Nicotinamide protects against diet-induced body weight gain, increases energy expenditure, and induces white adipose tissue beiging. Mol. Nutr. Food Res. *65*, e2100111.

Meng, Y., Ren, Z., Xu, F., Zhou, X., Song, C., Wang, V.Y., Liu, W., Lu, L., Thomson, J.A., and Chen, G. (2018). Nicotinamide promotes cell survival and differentiation as kinase inhibitor in human pluripotent stem cells. Stem Cell Rep. *11*, 1347–1356.

Menoret, A., Buturla, J.A., Xu, M.M., Svedova, J., Kumar, S., Rathinam, V.A.K., and Vella, A.T. (2018). T cell-directed IL-17 production by lung granular gammadelta T cells is coordinated by a novel IL-2 and IL-1beta circuit. Mucosal Immunol. *11*, 1398–1407.

Mitchell, S.J., Bernier, M., Aon, M.A., Cortassa, S., Kim, E.Y., Fang, E.F., Palacios, H.H., Ali, A., Navas-Enamorado, I., Di Francesco, A., et al. (2018). Nicotinamide improves aspects of healthspan, but not lifespan, in mice. Cell Metab. *27*, 667–676.e4.

Morales Del Valle, C., Maxwell, J.R., Xu, M.M., Menoret, A., Mittal, P., Tsurutani, N., Adler, A.J., and Vella, A.T. (2019). Costimulation induces CD4 T cell antitumor immunity via an innate-like mechanism. Cell Rep *27*, 1434–1445.e3.

Mouchiroud, L., Houtkooper, R.H., Moullan, N., Katsyuba, E., Ryu, D., Canto, C., Mottis, A., Jo, Y.S., Viswanathan, M., Schoonjans, K., et al. (2013). The NAD(+)/Sirtuin pathway modulates longevity through activation of mitochondrial UPR and FOXO signaling. Cell *154*, 430–441.

Muralimohan, G., Rossi, R.J., Guernsey, L.A., Thrall, R.S., and Vella, A.T. (2008). Inhalation of Staphylococcus aureus enterotoxin A induces IFN-gamma and CD8 T cell-dependent airway and interstitial lung pathology in mice. J. Immunol. *181*, 3698–3705.

Murugina, N.E., Budikhina, A.S., Dagil, Y.A., Maximchik, P.V., Balyasova, L.S., Murugin, V.V., Melnikov, M.V., Sharova, V.S., Nikolaeva, A.M., Chkadua, G.Z., et al. (2020). Glycolytic reprogramming of macrophages activated by NOD1 and TLR4 agonists: No association with proinflammatory cytokine production in normoxia. J. Biol. Chem. *295*, 3099–3114.

O'Neill, L.A., Kishton, R.J., and Rathmell, J. (2016). A guide to immunometabolism for immunologists. Nat. Rev. Immunol. *16*, 553–565.

Okano, T., Saegusa, J., Nishimura, K., Takahashi, S., Sendo, S., Ueda, Y., and Morinobu, A. (2017). 3-bromopyruvate ameliorate autoimmune arthritis by modulating Th17/Treg cell differentiation and suppressing dendritic cell activation. Sci. Rep. *7*, 42412.

Patel, C.H., Leone, R.D., Horton, M.R., and Powell, J.D. (2019). Targeting metabolism to regulate immune responses in autoimmunity and cancer. Nat. Rev. Drug Discov. *18*, 669–688.

Peled, T., Shoham, H., Aschengrau, D., Yackoubov, D., Frei, G., Rosenheimer, G.N., Lerrer, B., Cohen, H.Y., Nagler, A., Fibach, E., et al. (2012). Nicotinamide, a SIRT1 inhibitor, inhibits differentiation and facilitates expansion of hematopoietic progenitor cells with enhanced bone marrow homing and engraftment. Exp. Hematol. *40*, 342–355.e1.

Peng, M., Yin, N., Chhangawala, S., Xu, K., Leslie, C.S., and Li, M.O. (2016). Aerobic glycolysis promotes T helper 1 cell differentiation through an epigenetic mechanism. Science *354*, 481–484.

Qiu, J., Villa, M., Sanin, D.E., Buck, M.D., O'Sullivan, D., Ching, R., Matsushita, M., Grzes, K.M., Winkler, F., Chang, C.H., et al. (2019). Acetate promotes T cell effector function during glucose restriction. Cell Rep. *27*, 2063–2074.e25.

Rajman, L., Chwalek, K., and Sinclair, D.A. (2018). Therapeutic potential of NAD-boosting molecules: the in vivo evidence. Cell Metab *27*, 529–547.

Rao, R.R., Li, Q., Odunsi, K., and Shrikant, P.A. (2010). The mTOR kinase determines effector versus memory CD8+ T cell fate by regulating the expression of transcription factors T-bet and Eomesodermin. Immunity *32*, 67–78.

Rehman, I.U., Ahmad, R., Khan, I., Lee, H.J., Park, J., Ullah, R., Choi, M.J., Kang, H.Y., and Kim, M.O. (2021). Nicotinamide ameliorates amyloid beta-induced oxidative stress-mediated neuroinflammation and neurodegeneration in adult mouse brain. Biomedicines *9*, 408.

Saxton, R.A., and Sabatini, D.M. (2017). mTOR signaling in growth, metabolism, and disease. Cell *168*, 960–976.

Scatozza, F., Moschella, F., D'Arcangelo, D., Rossi, S., Tabolacci, C., Giampietri, C., Proietti, E., Facchiano, F., and Facchiano, A. (2020). Nicotinamide inhibits melanoma in vitro and in vivo. J. Exp. Clin. Cancer Res. *39*, 211.

Shackelford, D.B., and Shaw, R.J. (2009). The LKB1-AMPK pathway: metabolism and growth control in tumour suppression. Nat. Rev. Cancer *9*, 563–575.

Song, S.B., Park, J.S., Jang, S.Y., and Hwang, E.S. (2021). Nicotinamide treatment facilitates mitochondrial fission through Drp1 activation mediated by SIRT1-induced changes in cellular levels of cAMP and Ca(2). Cells *10*, 612.

Su, C.F., Liu, D.D., Kao, S.J., and Chen, H.I. (2007). Nicotinamide abrogates acute lung injury caused by ischaemia/reperfusion. Eur. Respir. J. *30*, 199–204.

Svedova, J., Menoret, A., Mittal, P., Ryan, J.M., Buturla, J.A., and Vella, A.T. (2017). Therapeutic blockade of CD54 attenuates pulmonary barrier damage in T cell-induced acute lung injury. Am. J. Physiol. Lung Cell Mol. Physiol. *313*, L177–L191.

Tan, C.L., Chin, T., Tan, C.Y.R., Rovito, H.A., Quek, L.S., Oblong, J.E., and Bellanger, S. (2019). Nicotinamide metabolism modulates the proliferation/differentiation balance and senescence of human primary keratinocytes. J. Invest. Dermatol. *139*, 1638–1647.e3.

Teege, S., Hann, A., Miksiewicz, M., MacMillan, C., Rissiek, B., Buck, F., Menzel, S., Nissen, M., Bannas, P., Haag, F., et al. (2015). Tuning IL-2 signaling by ADP-ribosylation of CD25. Sci. Rep. *5*, 8959.

Tran, M.T., Zsengeller, Z.K., Berg, A.H., Khankin, E.V., Bhasin, M.K., Kim, W., Clish, C.B., Stillman, I.E., Karumanchi, S.A., Rhee, E.P., et al. (2016). PGC1alpha drives NAD biosynthesis linking oxidative metabolism to renal protection. Nature *531*, 528–532.

Tsurutani, N., Mittal, P., St Rose, M.C., Ngoi, S.M., Svedova, J., Menoret, A., Treadway, F.B., Laubenbacher, R., Suarez-Ramirez, J.E., Cauley, L.S., et al. (2016). Costimulation endows immunotherapeutic CD8 T cells with IL-36 responsiveness during aerobic glycolysis. J. Immunol. *196*, 124–134.

Tyrakis, P.A., Palazon, A., Macias, D., Lee, K.L., Phan, A.T., Velica, P., You, J., Chia, G.S., Sim, J., Doedens, A., et al. (2016). S-2-hydroxyglutarate regulates CD8(+) T-lymphocyte fate. Nature *540*, 236–241.

Ungerstedt, J.S., Blomback, M., and Soderstrom, T. (2003). Nicotinamide is a potent inhibitor of proinflammatory cytokines. Clin. Exp. Immunol. *131*, 48–52.

Van Gool, F., Galli, M., Gueydan, C., Kruys, V., Prevot, P.P., Bedalov, A., Mostoslavsky, R., Alt, F.W., De Smedt, T., and Leo, O. (2009). Intracellular NAD levels regulate tumor necrosis factor protein synthesis in a sirtuin-dependent manner. Nat. Med. *15*, 206–210.

Watts, T.H. (2005). TNF/TNFR family members in costimulation of T cell responses. Annu. Rev. Immunol. *23*, 23–68.

Yoshino, M., Yoshino, J., Kayser, B.D., Patti, G.J., Franczyk, M.P., Mills, K.F., Sindelar, M., Pietka, T., Patterson, B.W., Imai, S.I., et al. (2021). Nicotinamide mononucleotide increases muscle insulin sensitivity in prediabetic women. Science *372*, 1224–1229.

Yu, Y.R., Imrichova, H., Wang, H., Chao, T., Xiao, Z., Gao, M., Rincon-Restrepo, M., Franco, F., Genolet, R., Cheng, W.C., et al. (2020). Disturbed mitochondrial dynamics in CD8(+) TILs reinforce T cell exhaustion. Nat. Immunol. *21*, 1540–1551.

Zhang, Q., Li, J., Zhong, H., and Xu, Y. (2021). The mechanism of nicotinamide on reducing acute lung injury by inhibiting MAPK and NF-kappaB signal pathway. Mol. Med. *27*, 115.

Zheng, M., Cai, J., Liu, Z., Shu, S., Wang, Y., Tang, C., and Dong, Z. (2019). Nicotinamide reduces renal interstitial fibrosis by suppressing tubular injury and inflammation. J. Cell Mol. Med. *23*, 3995–4004.

Zhou, B., Wang, D.D., Qiu, Y., Airhart, S., Liu, Y., Stempien-Otero, A., O'Brien, K.D., and Tian, R. (2020). Boosting NAD level suppresses inflammatory activation of PBMCs in heart failure. J. Clin. Invest. *130*, 6054–6063.

## STAR★METHODS

### KEY RESOURCES TABLE

| REAGENT or RESOURCE | SOURCE | IDENTIFIER |
|---|---|---|
| Antibodies | | |
| Rat monoclonal α-CD134 | BioXCell | Cat# BE0031; RRID:AB_1107592 |
| Rat monoclonal α-CD137 | BioXCell | Cat# BE0239; RRID:AB_2687721 |
| Rabbit monoclonal α-pAMPK (Thr172) | Cell Signaling Technologies | Cat# 2535; RRID:AB_331250 |
| Rabbit monoclonal α-AMPK | Cell Signaling Technologies | Cat# 5832; RRID:AB_10624867 |
| Rabbit monoclonal α-pmTOR (Ser2448) | Cell Signaling Technologies | Cat# 5536; RRID:AB_10691552 |
| Rabbit monoclonal α-mTOR | Cell Signaling Technologies | Cat# 2983; RRID:AB_2105622 |
| Rabbit polyclonal α-β-Actin | Sigma-Aldrich | Cat# A5060; RRID:AB_476738 |
| Rat monoclonal α-CD4 | BD Biosciences | Cat# 552775; RRID:AB_394461 |
| Rat monoclonal α-CD8a | BD Biosciences | Cat# 558106; RRID:AB_397029 |
| Hamster monoclonal α-TCR Vβ3 (KJ25) | BD Biosciences | Cat# 743413; RRID:AB_2741486 |
| Rat monoclonal α-TCR Vβ14 (14-2) | BD Biosciences | Cat# 553257; RRID:AB_394737 |
| Rat monoclonal α-IFNγ (XMG1.2) | Thermo Fisher Scientific | Cat# 45-7311-82; RRID:AB_1107020 |
| Rat monoclonal α-CD44 (IM7) | BD Biosciences | Cat# 559250; RRID:AB_398661 |
| Rat monoclonal α-CD62L (MEL-14) | Thermo Fisher Scientific | Cat# 12-0621-82; RRID:AB_465721 |
| Mouse monoclonal α-pS6 (Ser235, Ser236) | Thermo Fisher Scientific | Cat# 12-9007-42; RRID:AB_2572667 |
| Mouse monoclonal α-CD8 | BD Biosciences | Cat# 341051; RRID:AB_400209 |
| Mouse monoclonal α-CD4 | BD Biosciences | Cat# 561840; RRID:AB_10895807 |
| Mouse monoclonal α-CD25 | | Cat# 565106; RRID:AB_2744339 |
| Chemicals, peptides, and recombinant proteins | | |
| Ova peptide SIINFEKL | Invivogen | Cat# vac-sin; CAS# 138831-86-4 |
| *Staphylococcus aureus (S. aureus)* enterotoxin A (SEA) | Toxin Technologies Inc. | Cat# AT101 |
| (hr)IL-2 | NIH | N/A |
| Ionomycin (i) | Invivogen | Cat# inh-ion; CAS# 56092-82-1 |
| Phorbol 12-Myristate 13-Acetate (PMA) | Sigma-Aldrich | Cat# 554400; CAS# 16561-29-8 |
| Nicotinamide (NAM) | Sigma-Aldrich | Cat# 72340; CAS# 98-92-0 |
| Nicotinamide adenine dinucleotide ($NAD^+$) | Sigma-Aldrich | Cat# N1511; CAS# 53-84-9 |
| FK866 | Selleck | Cat# S2799; CAS# 658084-64-1 |
| EX-527 | Selleck | Cat# S1541; CAS# 49843-98-3 |
| IL-12 | R&D Systems | Cat# 419-ML/CF |
| IL-33 | R&D Systems | Cat# 3626-ML/CF |
| IL36β | R&D Systems | Cat# 7060-ML/CF |
| LIVE/DEAD™ Fixable Blue Dead Cell Stain Kit | Invitrogen | Cat# L34962 |
| CellTrace™ Violet Cell Proliferation Kit | Invitrogen | Cat# C34557 |
| Critical commercial assays | | |
| Dynabeads™ Untouched™ Mouse CD8 Cells Kits from ThermoFisher Scientific | Thermo Fisher Scientific | Cat# 11417D |
| Dynabeads™ Mouse T-Activator CD3/CD28 for T-Cell Expansion and Activation | Thermo Fisher Scientific | Cat# 11452D |
| Lympholyte®-M | Cederlane | Cat# CL5030 |
| Lympholyte®-H | Cederlane | Cat# CL5020 |
| Foxp3/Transcription Factor Staining Buffer Set | Thermo Fisher Scientific | Cat# 00-5523-00 |

(*Continued on next page*)

*Continued*

| REAGENT or RESOURCE | SOURCE | IDENTIFIER |
|---|---|---|
| Mouse IL-2 ELISA Set | BD Biosciences | Cat# 555148; RRID:AB_2869030 |
| Mouse IFNγ ELISA Set | BD Biosciences | Cat# 555138; RRID:AB_2869028 |
| LEGENDplex™ Mouse Inflammation Panel | BioLegend | Cat# 740150 |
| Human IFN-gamma Quantikine ELISA Kit | R&D Systems | Cat# SIF50C |
| iScript™ cDNA Synthesis Kit | BioRad | Cat# 1708891 |
| Seahorse Gycolysis stress test kit | Agilent Technologies | Cat# 103020-100 |
| Seahorse XFp Media | Agilent Technologies | Cat# 103575-100 |
| Seahorse XFe96 FluxPak mini | Agilent Technologies | Cat# 102601-100 |
| Experimental models: Organisms/strains | | |
| C57BL/6J | The Jackson Laboratory | JAX: 000664 |
| C57BL/6J Rag$^{-/-}$ OT-I CD45.1 | University of Washington | N/A |
| Human Peripheral Blood Mononuclear Cells | Stem Cells | Cat# 70025 |
| Oligonucleotides | | |
| Primers for qPCR, see Table S1 | see Table S1 | N/A |
| Software and algorithms | | |
| FlowJo v10.6.1 | FlowJo | RRID: SCR_008520 |
| GraphPad Prism v9 | GraphPad | RRID: SCR_00279 |
| Sciex® OS software v.2.0.1 | Sciex | https://sciex.com/products/software/sciex-os-software |
| LEGENDplex software | BioLegend | https://sciex.com/products/software/sciex-os-software |
| Gene Tools | Syngene | https://www.syngene.com/software/genetools-automatic-image-analysis/ |
| Seahorse Wave | Agilent Technologies | RRID:SCR_014526 |

## RESOURCE AVAILABILITY

### Lead contact

Further information and requests for resources and reagents should be directed to and will be fulfilled by the lead contact, Anthony T. Vella (vella@uchc.edu).

### Materials availability

This study did not generate new unique reagents.

### Data and code availability

Data reported in this paper will be shared by the lead contact upon request. This paper does not report original code. Additional information and data reported in this paper is available from the lead contact upon request.

## EXPERIMENTAL MODEL AND SUBJECT DETAILS

### Mice and adoptive transfer

Male and female C57BL/6J mice (6–9 weeks old) were purchased from the Jackson Laboratory (Bar Harbor, ME). CD45.1$^{+}$ RAG$^{-/-}$ OT-I TCR transgenic mice were bred in-house. All mice were maintained in the UConn Health animal facility. All animal procedures were approved by the UConn Health Institutional Animal Care and Use Committee and performed in accordance with National Institutes of Health Animal Care and Use Guidelines. Spleen and lymph node preparations from CD45.1$^{+}$ RAG$^{-/-}$ OT-I transgenic mice containing 5 × 10$^{5}$ CD8$^{+}$ T cells expressing T cell receptor Vα2 Vβ5 and specific to Ova peptide SIINFEKL were adoptively transferred into CD45.2$^{+}$ C57BL/6J mice. The following day, recipients were immunized intraperitoneally (i.p.) with 50 μg SIINFEKL peptide (InvivoGen, San Diego, CA) and 20 μg α-CD134

(clone OX86, Bio X Cell, Lebanon, NH) plus 10 μg of α-CD137 (clone 3H3, Bio X Cell, Lebanon, NH) agonists (Lee et al., 2004; Tsurutani et al., 2016).

### *In vitro* and *ex vivo* cell culture

For *in vitro* cultures, naïve $CD3^+$, $CD4^+$, $CD8^+$ T cells from spleen and lymph nodes (inguinal, brachial, axillary and cervical) of male and female C57BL/6J mice (6–9 weeks old) were purified by negative selection using Dynabeads™ Untouched™ Mouse Cells Kits from ThermoFisher Scientific (Waltham, MA). Cells were then differentiated *in vitro* using Dynabeads™ Mouse T-Activator CD3/CD28 for T cell Expansion and Activation from ThermoFisher Scientific (1:1 ratio) (Waltham, MA), plus hrIL-2 (30 U/ml), in the presence or absence of NAM 30 mM or 10 mM. After 66 h live cells were recovered using Lympholyte®-M from Cederlane (Burlington, NC) as per manufacturer's instructions. Lastly, cells were restimulated using either Dynabeads™ Mouse T-Activator CD3/CD28 or PMA + ionomicyn (PMAi). For *ex-vivo* cultures, *in vivo*–primed $CD8^+$ T cells from spleen and lymph nodes (inguinal, brachial, axillary and cervical) were purified by negative selection using Dynabeads™ Untouched™ Mouse CD8 Cells Kit from ThermoFisher Scientific (Waltham, MA) following biotinylated α-CD45.2 Ab from ThermoFisher Scientific (Waltham, MA). Cells were then restimulated using SIINFEKL, PMAi or IL-2/IL-12 plus IL-33 or IL-36β (R&D Systems, Minneapolis, MN) for the indicated time points.

### Human cells

Peripheral blood mononuclear cells (PBMCs) (STEMCELL Technologies, Vancouver, Canada) from male healthy donors (25–32 years old) were cultured at $2.25 \times 10^6$ cells/ml in complete T cell media: RPMI 1640 (ATCC 30–2001), 2 mM L-glutamine, 10 mM HEPES, 1 mM sodium pyruvate, 4500 mg/L glucose, and 1500 mg/L sodium bicarbonate, 1x antibiotic-antimycotic (Gibco), 1x non-essential amino acids (Gibco) and 10 ng/ml recombinant human IL-2 (R&D Systems, Minneapolis, MN). Products were obtained using Institutional Review Board (IRB) approved consent forms and protocols. Cells were stimulated with α-CD3/CD28 Dynabeads (Gibco) for 6 days at a 1:1 ratio of cells:beads unless otherwise noted. After 6 days, viable cells were purified using Lympholyte®-H (Cedar Lane, Burlington, NC). Cells were restimulated for 6 h with α-CD3/CD28 Dynabeads.

## METHODS DETAILS

### *S. aureus* enterotoxin A immunization and diet

Male and female C57BL/6J mice (6–9 weeks old) were fed with a control diet or diet supplemented with NAM (125 mg/day/Kg) (Research Diet Inc, New Brunswick, NJ) for 14 days before immunization. On day 14 mice were anesthetized with isoflurane (Vedco Inc., Saint Joseph, MO) and given 1 μg of *S. aureus* enterotoxin A diluted in 50 μL of PBS, or PBS alone by intranasal (i.n.) route (Kumar et al., 2013). Serum was collected 6 h post immunization. Mice continued on the control and NAM supplemented diet for two more days, and then sacrificed. Axillary and brachial lymph nodes (LN) were collected and the isolated LN cells were analyzed by flow cytometry. To measure intracellular IFNγ, cells were restimulated *in vitro* with 0.1 μg *S. aureus* enterotoxin A for 4 h and analyzed by flow cytometry.

### Flow cytometry

Single cell suspensions were washed, resuspended in FACS buffer (HBSS, 0.1% sodium azide and 3% fetal calf serum), kept on ice, and treated with FcR blocking solution for 30 min at 4°C with mAbs: α-CD8 (BD Biosciences, Franklin Lakes, NJ), α-CD4 (BD Biosciences, Franklin Lakes, NJ), α-Vβ3 (BD Biosciences, Franklin Lakes, NJ), α-Vβ14 (BD Biosciences, Franklin Lakes, NJ) and α-CD45.1 (ThermoFisher Scientific, Waltham, MA). Live cells were gated using LIVE/DEAD™ Fixable Blue Dead Cell Stain Kit from ThermoFisher Scientific (Waltham, MA). For phospho (p) S6 detection, cells were washed with FACS buffer and further processed for intracellular staining using the Foxp3 fixation/permeabilization buffer (eBioscience, Waltham, MA) as per the manufacturer's instructions. The fixed and permeabilized cells were then incubated with the Phospho-S6 (Ser235, Ser236) antibody from ThermoFisher Scientific (Waltham, MA) and diluted in 1x permeabilization buffer overnight at 4°C. For IFNγ detection, cells were washed with FACS buffer, fixed with paraformaldehyde (Sigma-Aldrich, St. Louis, MO), permeabilized with saponin (Sigma-Aldrich, St. Louis, MO) and then incubated with the IFNγ antibody from ThermoFisher Scientific (Waltham, MA) followed by dilution in 1x permeabilization buffer overnight at 4°C. Sample were washed twice with 1x permeabilization buffer, and resuspended with FACS buffer. For human cells the following mAbs were used: α-CD8 (clone RPA-T8), α-CD4 (clone RPA-T4) and α-CD25 (clone M-A251) from BD Biosciences

(Franklin Lakes, NJ). Cells staining events were acquired on a LSRII analyzer (BD Biosciences, Franklin Lakes, NJ) using DIVA software. Data were analyzed using FlowJo software (FlowJo, LLC, Ashland, OR).

### Quantitative real-time RT-PCR

Total RNA was extracted using the miRNeasy mini kit (Qiagen, Valencia, CA) and reverse-transcribed with an iScript cDNA synthesis kit (Bio-Rad, Hercules, CA). Real-time quantitative PCR measurement of cDNA was then performed using SsoAdvanced Universal SYBR® Green Supermix (Bio-Rad, Hercules, CA) and a CFX96 real-time PCR instrument (Bio-Rad, Hercules, CA). All primers are listed in Table S1. Each sample was run in duplicate and gene expression levels were normalized to β-actin as housekeeping gene. Relative mRNA expressions were calculated using the $2^{-\Delta\Delta}$t method (Livak and Schmittgen, 2001).

### Cytokine secretion analysis

Supernatants from cell cultures were spin (400 g, 10 min), and cytokine levels were measured using the LEGENDplex multi-analyte flow assay kits (BioLegend, San Diego, CA) as per manufacturer's instructions. Data were collected on the ZE5 Cell analyzer (Bio-Rad, Hercules, CA) and analyzed using LEGENDplex™ Data Analysis Software Suite (BioLegend, San Diego, CA). Mouse IFNγ and IL-2 ELISA kit were purchased from BD Bioscience (San Jose, CA) and human IFNγ was measured with the ELISA kit from R&D Systems (Minneapolis, MN).

### Immunoblotting

Cells were lysed with NE-PER Nuclear and Cytoplasmic Extraction Reagent Kit (ThermoFisher Scientific, Waltham, MA) for nuclear and cytoplasmic extractions, according to the manufacturer's instructions. Lysates were resuspended in Laemmli buffer (50 mm Tris–Cl, pH 6.8, 10% glycerol, 2% SDS, 0.1% bromophenol blue, 5% 2-mercaptoethanol), boiled for 5 min, separated on 4–20% polyacrylamide gels (Bio-Rad, Hercules, CA), transferred to nitrocellulose membranes (Bio-Rad, Hercules, CA), blocked, and probed with the following antibodies: phospho-mTOR (Ser2448), mTOR, phospho-AMPK (Thr172), AMPK, phospho-p65 (Ser536), p65 and HDAC1 from Cell Signaling (Danvers, MA), β-Actin from Sigma-Aldrich (St. Louis, MO). Membranes were developed using an ECL plus chemiluminescence kit (ThermoFisher Scientific, Waltham, MA) and protein quantification was performed using the GeneTool software (Syngene, Frederick, MD).

### Glycolysis assay

Purified $CD8^+$ OT-I T cells ($3 \times 10^5$/well) were plated in 96-well Seahorse plates (Seahorse Bioscience, North Billerica, MA) previously coated with Cell-Tak (BD Biosciences, Franklin Lakes, NJ). Extracellular acidification rates (ECAR) were measured using an XF-96 extracellular flux analyzer and a glycolysis stress test kit as per the manufacturer's instructions (Agilent, Santa Clara, CA).

### NAM and $NAD^+$ metabolite measurement

Samples were agitated and 100 μL of each sample (including quality control samples) were measured and spiked with 5 μL internal standard solution followed by the addition of 100 μL of 70:30 cold ethanol/water. Samples were vortexed for 10 min at 2,500 RPM and centrifuged for 10 min at 14,000 RPM. The collected supernatant was transferred to an analytical vial and analyzed by UHPLC-QTOF HRMS. Quality control and actual samples were analyzed using a Sciex® Exion UHPLC coupled with an Sciex® X500R™ Quadrupole/Time of Flight (AB Sciex., Framingham, MA). An ACE® 5AQ C18 (5 μm, 4.6 × 50 mm) column, maintained at 30°C and with a sample injection volume of 5 μL on a 20 μL loop, was utilized for analyte separation. The mobile phase, consisted of 0.1% formic acid in water (solvent A) and 0.1% formic acid in acetonitrile (solvent B), was employed for gradient column elution. The total run time was 5.0 min with a constant flow rate of 0.6 mL/min. The detection and quantification of analytes and internal standard were performed in positive ESI + MRMHR™ mode. The Sciex® OS software was utilized for guided analyte signal optimization. Statistical analysis for obtaining calibration and quantification results for all compounds was performed using Analytics™, which is included in the Sciex® OS software v.2.0.1.

## QUANTIFICATION AND STATISTICAL ANALYSIS

A two-tailed Student's unpaired *t* test was used for two-group comparisons, a one-way Anova with Tuckey's post-hoc test was used when three or more groups were compared. ECAR curves were compared using the area under the curve (AUC) method (Falconer et al., 2021; Murugina et al., 2020). When combination of

independent experiments are shown data are means ± SEM. When a representative experiment is shown, data are means of technical replicates ± SD. Values of $p < 0.05$ (*) were used as significant threshold; $p < 0.01$ is indicated as (**) and $p < 0.001$ as (***). All statistical analysis were processed by the GraphPad Prism Version 9.0 software package (GraphPad Software, San Diego, CA).